A STOCHASTIC DROPLET IMPINGEMENT MODEL TO PREDICT THE SURFACE STRUCTURES, LOCAL DENSITIES AND LUDLAM LIMIT OF RIME ACCRETIONS.

Pierre McComber
Ecole de technologie supérieure
Montréal, (Québec)

Yves Turgeon
Université du Québec à Chicoutimi
Chicoutimi, (Québec)

ABSTRACT

A stochastic droplet impingement model for soft rime accretion on a wire is used to evaluate the surface structure as measured by the fractal dimension, local rime density and Ludlam limit (the limit between dry and wet growth) on a cylindrical shape. This two-dimensional model calculates trajectories of successive droplets originating from a randomly chosen point at a large distance from a two-dimensional cylinder. The equation of movement of each droplet is integrated to find the trajectories resulting from the action of the air drag force. The droplet are assumed to freeze as they impinge on the surface of the wire or of previously formed ice. The simulated soft rime accretions are then analyzed numerically to determine the fractal dimension of the contour. High correlation coefficients indicate good fractal properties of the accretion surface. An estimate of the rime local density is calculated from the simulation results. The local Ludlam limit is also verified to provide a limit in the use of the dry growth assumptions.

INTRODUCTION

Atmospheric ice accretion on structures is a major design factor for overhead transmission lines in northern regions. The complexity of the ice accretion process and the scarcity of accretion data make it interesting to develop a simulation model in order to predict both static and aerodynamic loads on transmission lines.

Ice accretion models applicable to this problem have been developed Ackley and Tempelton (1979), Lozowski et al. (1984), McComber (1984)) and Makkonen (1984). These models assume the water to be locally evenly distributed on the surface while solidifying. This is a reasonable assumption for hard rime modelling, but not for softer rime. In mountains (altitude > 400 m) where in-cloud icing occurs most frequently, soft rime of various densities is formed in most instances and a better model is still required for this type of atmoshpheric ice.

In Fig. 1 is shown typical soft rime accretion obtained at an altitude of 902 m. It can be seen that the rime is forming in very small branches or feathers in a process that is highly history-dependent. This type of ice is characterized by the rapid freezing of droplets where they impact on the accretion surface. Therefore it appears more realistic to simulate the trajectories of droplets randomly distributed in space, then find the impingement site on the accretion and consider that the frozen droplet becomes part of the accretion at that location. Since the accretion growth will be dependent on the random distribution of droplets in space it is called a stochastic model and is more appropriate to predict the characteristics of soft rime.

Before attempting to compare the rime simulation with ice collected in the field, it is essential to estimate and quantify certain characteristics of the random shape obtained.

Three types of parameters associated with the two-dimensional simulated rime accretions were investigated by computer and the results are presented in this paper. First the surface structure is measured by the calculation of the fractal dimension of the contour. Then an attempt is made to evaluate the local accretion density by the water volumetric fraction. And finally the Ludlam limit is calculated locally by a surface heat balance in order to predict the region where there is a change from hard to soft rime.

Figure 1. Photograph of a soft rime accretion taken At Mont Valin (902 m)

NUMERICAL SIMULATION OF RIME ACCRETION ON STRUCTURES

The soft rime is first simulated in two dimensions by integrating the equations of movement to determine the individual trajectories. Droplet trajectories were first calculation by Langmuir and Blottget (1946) to find the collection efficiency of a structure. For the soft rime model, droplets are first generated randomly located in space with equal probabilities. They originate at a large distance from the cable surface modelled by a two dimensional cylinder. The equation of movement for these droplets is integrated by a Runge-Kutta scheme to yield their velocity and the position as they approach and impinge on the accretion.

In undimensional form this equation of movement is written (McComber, 1984):

$$K \frac{D\vec{V}}{Dt} = \frac{Cd\ Re}{24} (\vec{V} - \vec{U}) \qquad (1)$$

In Eq. 1 the derivative $D\vec{V}/Dt$ is Lagrangian i.e. taken following the droplet. K is the Stokes number, $\vec{V} = v / u_o$ the undimensional droplet velocity and $U = u / u_o$ the air velocity. The reference velocity u_o (m/s) is taken far from the obstacle where the air and droplets are assumed to have the same constant speed. Cd is the drag coefficient and Re is the droplet Reynolds number.

The inertia parameter or Stokes number is defined by:

$$K = \frac{2a^2 \rho_w u_o}{9 \mu C} \qquad (2)$$

In this expression C (m) is the cylinder radius, a (m) the droplet radius, μ (kg/m.s)

the absolute viscosity of air and ρ_w (kg/m^3) the droplet density.

The empirical evaluation of the droplet drag as determined by Beard and Pruppacher (1969) is used to find the air drag on the droplet. The air velocity is calculated by the solution of a potential flow around the cylinder which is a realistic approach to simulate the flow outside the boundary layer on the upwind side of the cylinder. However, the effect of the accretion shape on the air flow around the iced cylinder is not taken into account. This is not very accurate for longer rime formation. There is no doubt that the accuracy of the potential flow solution could be improved by modelling larger accretion shapes as growing ellipses.

On impact each droplet of the accretion appears as a pixel on the computer screen and it is memorized in a screen matrix. For the simulation the ratio between the droplet diameter and the cylinder diameter is taken to be the same as the one being simulated.

Figures 2 and 3 show random trajectories plotted for increasing values of K. It can be observed from Fig. 2 and 3 that the important differences in trajectories occur for $0.5 < K < 4$. For $K < 0.5$ most of the droplets simply follow the air flow around the obstacle. For $K > 4$ they travel in straight lines undisturbed by the air stream deviation.

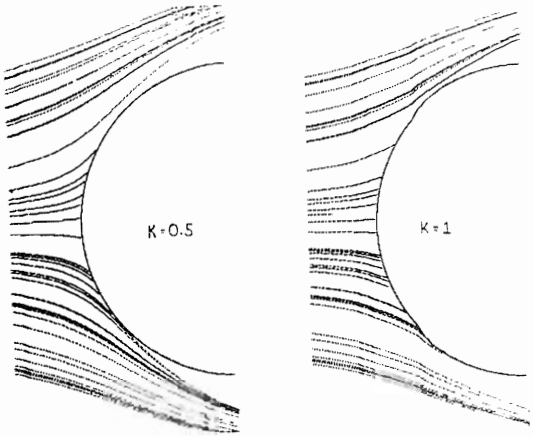

Figure 2. Droplets trajectories upstream of a cylinder for Stokes numbers of K = 0.5 and K = 1

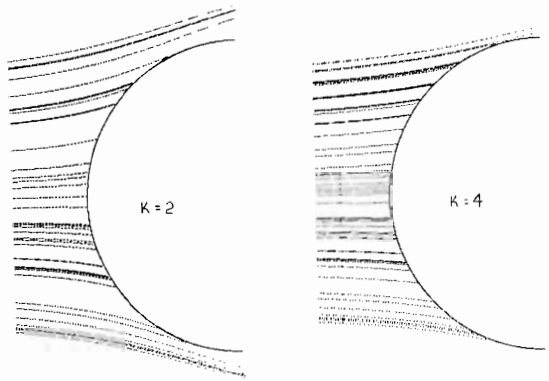

Figure 3. Droplets trajectories upstream of a cylinder for Stokes numbers of K = 2 and K = 4

RIME SIMULATION USING THE STOCHASTIC MODEL

For a stochastic simulation of atmospheric icing the accretion size depends on the number n_d of droplet trajectories calculated. However this simulation can be related to real time by the use of the appropriate meteorological parameters.

The first step in calculating the simulation time t_s is to find the mass flux of droplet impinging on the accretion surface. In general the intensity of accretion I (kg/m^2.s) for a cylinder is given by the following (Makkonen, 1984):

$$I = E\, u_o\, w \qquad (3)$$

where u_o (m/s) is the wind velocity, E the collection efficiency and w (kg/m^3) the water liquid content.

The collection efficiency is the ratio between the liquid mass impinging on the accretion surface and the liquid mass that would have impinged on the same surface with no deviation from the wind effect.

The mass flow of droplet m (kg/s) generated at a large distance from a cylinder of radius C can be calculated per unit depth as:

$$m_w = w\ u_o\ C\ 2a \tag{4}$$

Then the simulation time can be estimated by:

$$t_s = \frac{n_d\ m_d}{m_w} \tag{5}$$

where m_d is the droplet mass (g).

The local itensity of accretion j ($kg/m^2.s$) will be given by:

$$j = \frac{n_d\ m_w}{d\theta\ C\ 2a\ t_s} \tag{6}$$

where $d\theta$ is the angle for a cylinder surface element, which in turn will determine a local collection efficiency β on the cylinder surface:

$$\beta = \frac{j}{u_o\ w} \tag{7}$$

In Figures 4, 5 and 6 are shown successive shapes obtained by a stochastic simulation of soft rime accretion. Since in the computer simulation a pixel corresponds to the droplet size a, the cylinder size C is the main dimension controlling factor. In this case a ration of 1/350 was taken between droplet and cylinder diameters. This correspond to a droplet size of 28.6 μm in the case of a cylinder 10 mm in diameter. The simulation being a random process, it is not possible to reproduce twice exactly the same shape. In Fig. 4 is shown a simulation for a Stokes parameter value of K = 0.5, whereas in Figures 5 and 6 the successive shapes obtained for a K = 1 parameter are displayed.

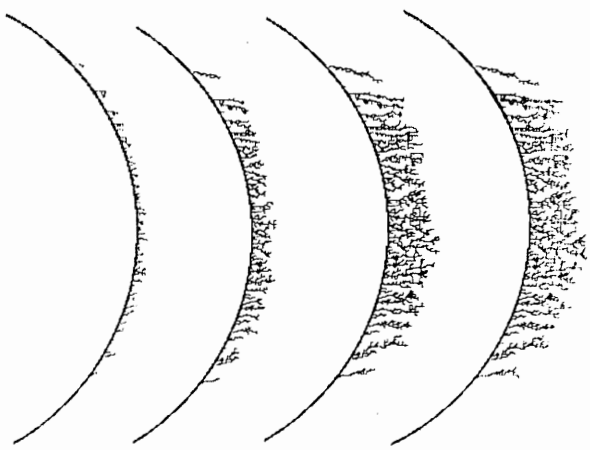

Figure 4. Simulation of rime with K = 0.5 for 500, 1500, 3000 and 4000 droplets

CALCULATION OF THE FRACTAL DIMENSION OF THE CONTOUR

The fractal dimension is a measure of the complexity of a shape. A straight line has a dimension of one. As the complexity of the line increases the fractal dimension also increases but remains less than two which is the dimension of an area.

Mandelbrot (1982) has contributed to the recent increase in popularity of the fractal dimensions by his study of various random shapes observed frequently in nature. In the case of the two-dimensional profile resulting from the stochastic simulation of rime accretion, fractal can be used to evaluate the complexity of the outside contour of the rime shape.

The measure of the fractal dimension can be done by computer once the two-dimensional contour has been previously digitized. The method as described in Fig. 7 consists in taking successive contour measurements, using each time a different length scale r_i. The number N_i of successive intersections of circles of radius r_i with the countour is counted. If the line has a more complex shape, taking a smaller r_i increases the number of intersection faster than that of a simple linear relationship. In fact this increase is dependent on the complexity of the contour.

Next, as illustrated in Fig. 8, the logarithm of N_i is plotted as a function of the logarithm of r_i to verify if the contour shape has the characteristics of a fractal dimension shape. If a straight line of negative slope is obtained with a high correlation coefficient on the log-log graph then the absolute value of the slope gives the fractal dimension D.

In order to apply this method to the rime shape a computer code was first developed to obtain the values of N_i for different values of r_i. Since part of the problem was to determine the right intersection of the circle r_i with the contour in the case of multiple intersections, the pixels forming the contour were first labelled with an increasing number. When two intersections were obtained the pixel with the smaller number indicated the right choice among the different possibilities.

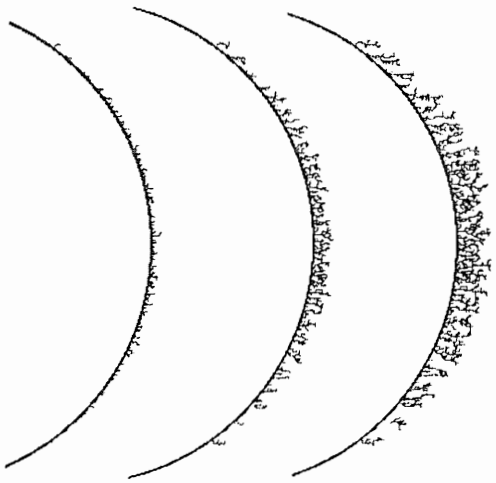

Figure 5. Simulation of rime formation with K = 1 for 500, 1500 and 3000 droplets

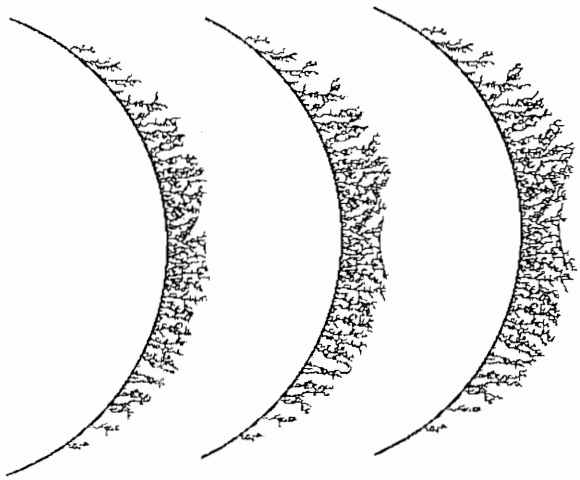

Figure 6. Simulation of rime formation with K = 1, y for 4000, 5000 and 6000 droplets

The computer code was first validated using the random shapes obtained by Nittman et al. (1985), while simulating a phenomenon called the viscous fingers growth. Their simulation was repeated and the random shapes obtained were tested to see if the same fractal dimension was obtained. A fractal dimension of 1.4162 was obtained as the average of 20 simulations. This value is indeed the same fractal dimension obtained by these authors. The computer code could thus be used with confidence on the rime contours themselves.

The best correlations for the fractal dimensions are obtained for simulation with the Stokes number K in the vicinity of one. In Table 1 is shown the average fractal dimension

and the correlation coefficients obtained for six simulations as a function of the number of droplets trajectories. For fewer droplets the fractal dimension is close to 1 since there is only a small modification of the cylinder surface. The fractal dimension increases for more droplets to a maximum of 1.65.

Table 1. Average of the fractal dimension for six simulations as a function of the number of droplets for K = 1.

Number of droplets	Fractal dimension	Correlation coefficient
500	1.04	0.999
2000	1.49	0.995
2500	1.52	0.996
3000	1.57	0.997
4000	1.65	0.998
5000	1.53	0.995

The correlation factors obtained for this series of simulations show that the contour does follow the fractal dimension law. However the fractal dimension obtained in each individual simulation depends on the exact shape and therefore vary slightly for each test.

Since K is the most important factor to determine trajectories tests were made for different values of K. The best fractal dimensions could be measured between K = 0.5 and 2. For higher or lower values the correlation was not as good. Figure 9 shows a summary of the results of the fractal dimension calculations.

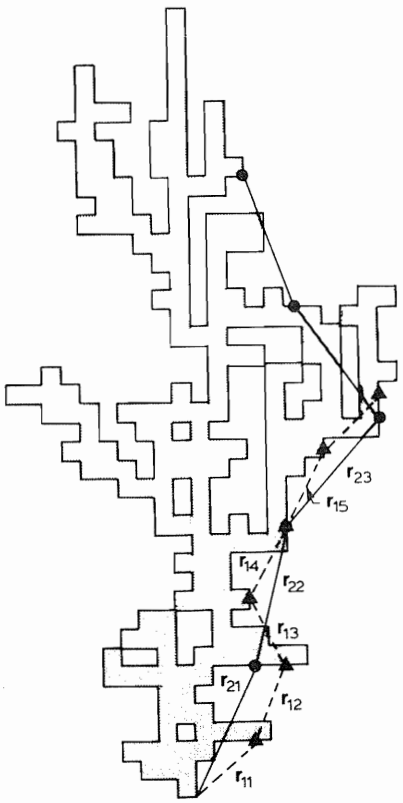

Figure 7. Measurements of shape contours with N_i intersections of circles of radius r_i

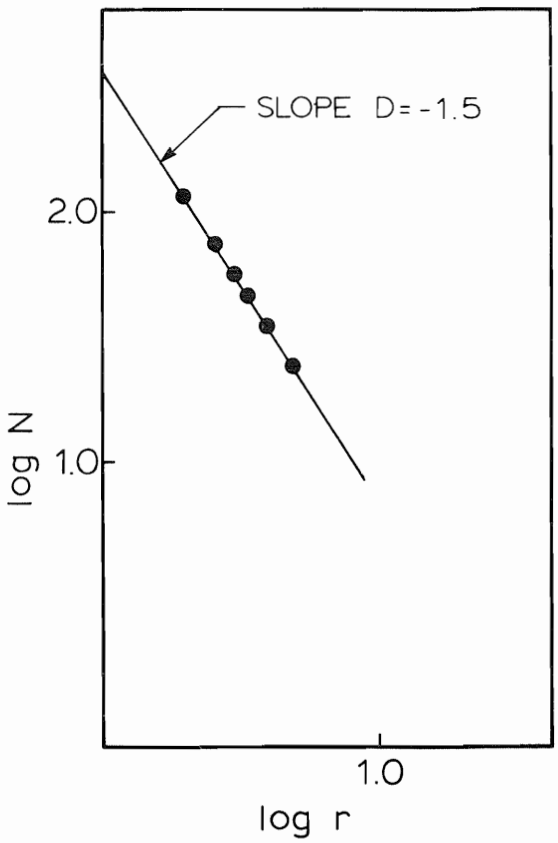

Figure 8. The number of intersections N_i as a function of the radius r_i and the calculation of the fractal dimension D from the slope

In this figure, the fractal dimension has the following characteristics. At the beginning of the rime accretion on the cylinder surface the fractal dimension increases with size. For accretions of medium size, lower fractal dimensions are obtained for higher inertia parameters. For larger accretions, fractal dimensions tend to be between 1.4 and 1.5.

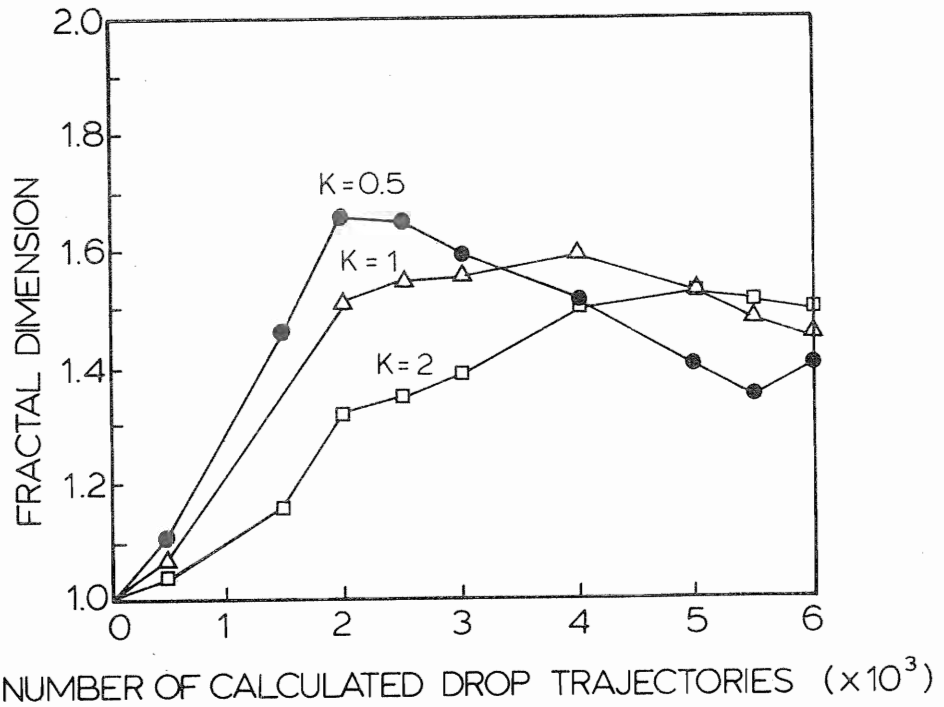

Figure 9. Fractal dimension as a function of calculated droplet trajectories for k = 0.5, 1 and 2

EVALUATION OF THE DENSITY FROM THE STOCHASTIC RESULTS

It has been observed that the density (Bain and Gayet, 1982) of rime tends to decrease on the side of a rime accretion i.e. with increasing angle from the stagnation point. The same type of observation could be made from the stochastic simulation Figures 4, 5 and 6. As the ice feathers grow droplets are prevented from reaching into the empty spaces. This will be more pronounced on the sides of the accretion. An attempt was made to estimate the density from the simulated shapes.

Since the size of a pixel is taken to be same as a droplet size the comparison of the accretion pixels to the total number of pixels including the voids will yield the water volumetric fraction:

$$\alpha = \frac{\text{number of droplet pixels}}{\text{total number of pixels part of the accretion}} \qquad (8)$$

This is illustrated in Fig. 10. However the density will be proportional to the water volumetric fraction at any location in the accretion. A comparison of the water volumetric fraction ratio is basically the same as a comparison of the density.

In order to determine a local density, as a function of the angle on the cylinder surface the ice accretion is first divided in 12 sectors by equally spaced lines parallel to the flow.

There is a difficulty in judging what is part of the accretion or not at the limit

between two sectors. Since the divisions are made along lines parallel to the flow the number of pixels in each row between a first accretion pixel in the row and the last one are considered to be part of the accretion whereas empty pixels before the first one, or after the last one are considered outside the accretion and are not counted.

In Fig. 11 the water volumetric fraction α is shown as a function of the angle θ from the stagnation point on the cylinder surface. It shows that there is no significant variations of the ice density with increasing angle, it tends to stay constant. The same observations were also made for different values of K and are not shown here. In Fig. 12 again for K = 1 the change in density was compared at different times during the same accretion simulation. In each sector of the accretion the water volumetric fraction is computed for successive 1000 droplets trajectories. In Fig. 12 the same pattern remains true. There is no significant variation of volumetric fraction with increasing angle on the cylinder surface.

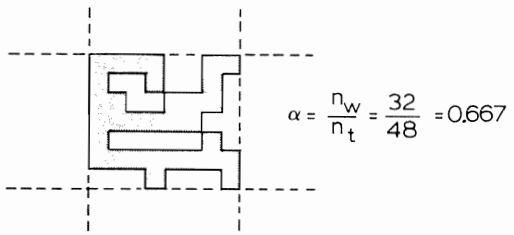

Figure 10. The calculation of the water volumetric fraction in a portion of the rime accretion.

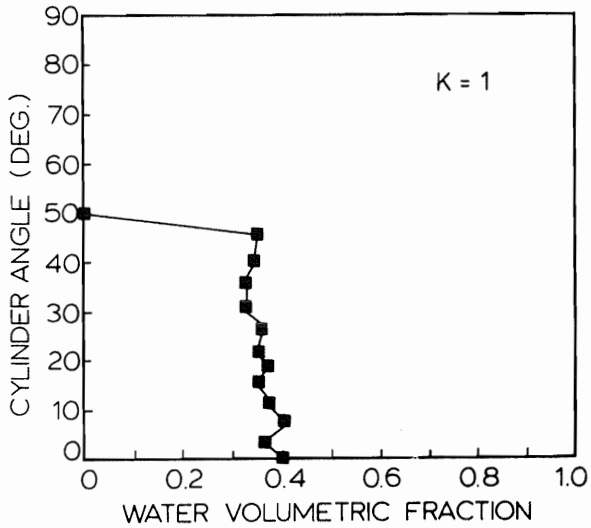

Figure 11. The water volumetric fraction as a function of the angle on the surface of an accretion for K = 1.

This indicates that this approach of density measurement does not account for the decrease in density on the sides and it may depend on how much of the empty spaces are considered as part of the accretion. However a more accurate description of the accretion boundaries is possible by counting pixels between successive contours instead of the sectors used above. This improvement of the method is not implemented at this point.

CALCULATION OF THE LOCAL LUDLAM LIMIT ON THE ACCRETION SURFACE

In order to freeze a droplet must first release its latent heat of fusion. At a certain level of icing intensity a droplet might not have time to freeze before another one impinges at the same location. If this is the case the second droplet coalesces forming a larger droplet. This results in the formation of a water film and is called wet growth. However since the collection efficiency varies with the angle on the cylinder surface, wet growth will occur first near the stagnation point resulting in harder rime at that site and softer rime on the sides. With the limit to dry growth calculated locally instead of globally for the whole accretion, the simulation could be made for both types of rime. The determination of the dry or wet regime is done through a heat balance on the accretion surface. The Ludlam limit (Ludlam, 1951) is defined as the critical water content we above which wet growth will be obtained.

Considering only the most important contributions to the heat balance (Personne et Gayet, 1984) on the surface the following equation is obtained:

$$Qf = Qc + Qw + Qe \tag{9}$$

where Qf (w/m^2) is the heat gain by the droplet freezing, Qc is the heat loss by convection to the ambiant air, Qw the heat loss to warm droplets to 0^oC, Qe is the heat loss by water evaporation.

The first term is obtained from the icing intensity I by:

$$Qf = I\ Lf \tag{10}$$

where I is the intensity of accretion ($kg/m^2.s$), and Lf the water latent heat of fusion (3.33×10 J/kg)

The heat loss by convection to ambiant air Qc is obtained by Newton's law of convection:

$$Qc = h\ (0^oC - ta) \tag{11}$$

where h ($W/m^2\ ^oC$) is the heat transfer coefficient by convection and ta is the air ambiant temperature. The heat transfer coefficient is evaluated by the relation between the Nusselt number and the Reynolds number for the flow around a cylinder:

$$h\ 2a\ /\ ka = (u_o\ 2a\ \rho\ /\ \mu) \tag{12}$$

ka (W/m^oC) is the thermal conductivity of the air. Eq. 12 gives an average heat transfer coefficient h, the local heat transfer coefficient, h_θ, is obtained from an interpolation curve to account for its variation as a function of the angle θ.

Qw the heat loss to warm droplets to zero^oC is given by:

$$Qw = I\ C_w\ (0^oC - ta) \tag{13}$$

in this equation Cw (J/kg^oC) is the specific heat of water.

Qe is the heat loss by evaporation and is given by the following relation (Personne et Gayet, 1984):

$$Qe = \frac{0.62\ h\ Le\ (e_o - e_a)}{C_p\ P_a} \tag{14}$$

where Cp ($J/kg/^oC$) is the specific heat heat of air, Le (2.257×10^6 J/kg) is the latent heat of evaporation, e_o is the saturated vapor pressure for water at 0^oC (610 Pa), e_a is the saturated water vapor pressure for water at t_a, Pa is the atmospheric pressure (101325 Pa).

By combining the previous Eqs. 7, 9, 10, 11, 13 and 14, for each sector of the cylinder surface it is possible to determine a critical liquid water content w_c, that separates wet from dry growth:

$$w_c\ (r) = \left[\frac{-t_a + \dfrac{0.62\ Le\ (e_o - e_a)}{C_p\ P_a}}{L_f + C_w\ t_a} \right] \frac{h_\theta}{\beta\ u_o} \tag{15}$$

Also this critical liquid water content will have the lowest value at the stagnation point where it is reffered to as w_o. Using a value of 25 mm for C and 14.9 μm for the droplet radius 5000 droplet trajectories were calculated per accretion. The simulation

time t_s can be calculated from the meteorological parameters using Eq. 5. Also an average was taken of three simulations for the upper and lower part of the cylinder making six samples available for each meteorological conditions. The cylinder surface was also divided in 31 sectors giving 15 sectors of six degrees on each side of the stagnation point. The critical liquid water content w_o computed for the stagnation point was compared with values in the litterature (Personne et Gayet, 1984) and were verified within a 10% difference. Using an undimensional representation w_c/w_o the critical angle θ_c, separating wet and dry growth, is plotted.

The results appear in Figures 13, 14 and 15 for K = 0.5, 1 and 2. For smaller K it takes a larger liquid water content w_c to achieve wet growth and the wet growth is more concentrated near the stagnation point. As K increases the wet growth extend to larger angles with less liquid water content.

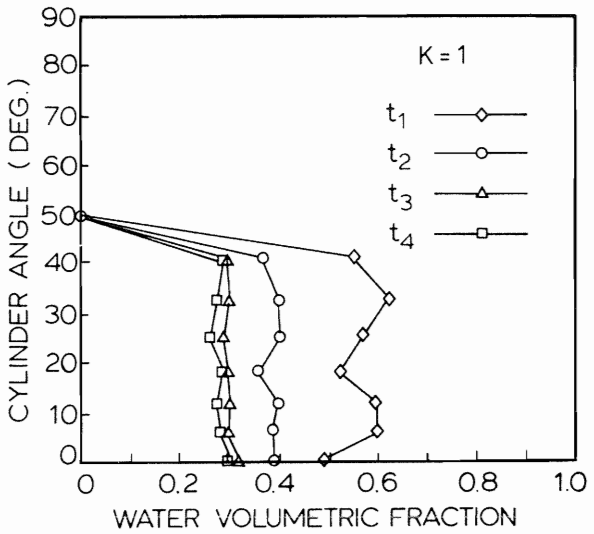

Figure 12. The different water volumetric fractions obtained as a function of the time of simulation and angle on the cylinder surface for K = 1.

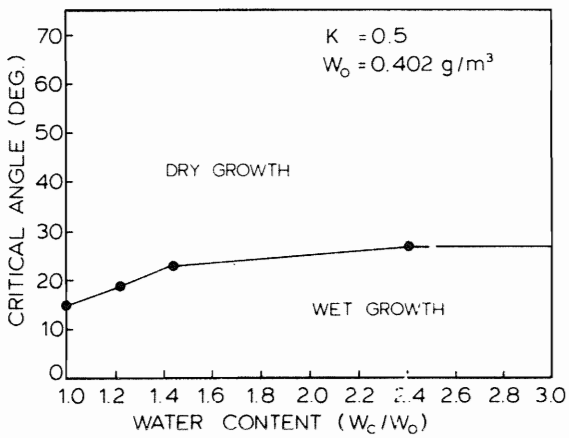

Figure 13. The critical angle for wet growth as a function of the undimensional liquid water content for K = 0.5 and 0.402 g/m^3

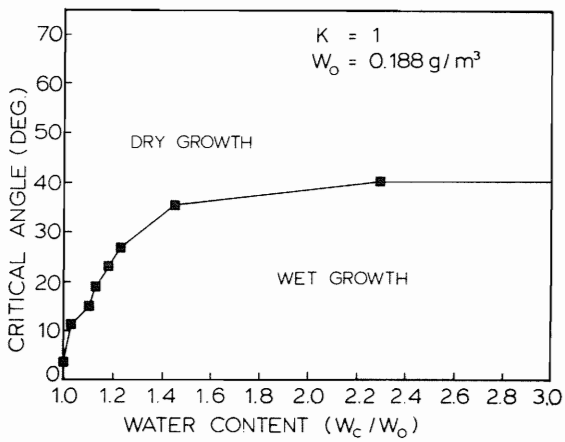

Figure 14. The critical angle for wet growth as a function of the undimensional liquid water content for K = 1 and w = 0.188 g/m^3

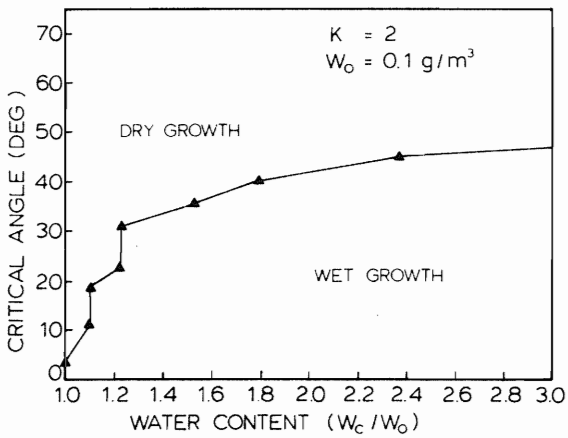

Figure 15. The critical angle for wet growth as a function of the undimensional liquid water content for K = 2 and w = 0.1 g/m^3

CONCLUSIONS

For soft rime, only a stochastic droplet impingement model can reproduce realistically the feather aspect of rime. This approach might be necessary for realistic simulation in the case of transmission line icing in high altitude regions where the wind speed encountered and the in-cloud conditions is likely to generate soft rime. Also it has been observed that for soft rime on flexible structures, as wires or cables, ice shedding is more prevalent and therefore should be included in a model.

The stochastic simulation of ice accretion has proven to consume large amount of computer time since each droplet trajectory must be individually calculated. However this type of approach is becoming more practical with the lower cost of computer time.

Two-dimensional rime shapes were generated on a cylindrical profile, and some characteristics of the simulation shapes were calculated by computer.

The fractal dimension of the accretion contour was first investigated. At the beginning of the rime accretion on a cable surface the fractal dimension increases with size. For accretions of medium size lower fractal dimensions are obtained for higher inertia parameters. For larger accretions, fractal dimensions tend to be between 1.4 and 1.5.

The water volumetric fraction of the accretion was estimated. However this approach to measure the accretion density could not account for the lower densities observed on the sides. This can be explained by the difficulty in accurately defining the boundary of the accretion which is essential to the evaluation of the density. The density might have large variations depending on the way the boundaries are chosen.

The local Ludlam limit was determined by the consideration of the heat balance at different angles on the accretion surface and the results can eventually be used to simulate more realistically a combination of hard and soft rime.

ACKNOWLEDGMENTS

This work is supported by the Conseil national de la Recherche in Science naturelle et en Génie du Canada (CRSNG) and by the Ministère de l'Education du Québec.

REFERENCES

Ackley, S.F. and Templeton, M.K. (1979), "Computer Modeling of Atmospheric Ice Accretion", CRREL Rept., 79-4 March.

Bain, M., Gayet, J.F., (1982), "Contribution to the Modeling of the Ice Accretion Process: Ice Density Variation with the Impacted Surface Angel", Ann. Glaciology, Vol. 4, pp 19-23.

Beard, K.V., Pruppacher, H.R. (1969), "A Determination of the Terminal Velocity and Drag of Small Water Drops by Means of a Wind Tunnel", J. Atmos. Sci., Vol. 26, pp 1066-1077.

Langmuir, I., Blodgett, K.B., (1946), "A Mathematical Investigation of Water Droplets Trajectories", Collected Works of I Langmuir, Vol X Pergamon Press., pp 383-393.

Lozowski E.P., Stallabrass J.R., Hearty, P.F. (1983), "The Icing of Unheated Nonrotating Cylinder. Part I: A Simulation Model" J. of Appl. Meteor., Vol 22 no 12, pp 2053-2062.

Ludlam, F.H., (1951), "The Heat Economy of a Rimed Cylinder", Quart J. Roy. Met. Soc., Vol 77, pp 663-666.

Makkonen, L., (1984), "Modeling of Ice Accretion on Wires", J. of Appl. Meteor., Vol 23, pp 929-939.

Mandelbrot, B., B., (1982), "The fractal Geometry of Nature", Freeman, New-York.

McComber, P., (1984), "Numerical Simulation of Cable Twisting Due to Icing", Cold Reg. Sc. & Techn., Vol 8, pp 253-259.

Nittman, Daccord, Stanley (1985), "Fractal Growth of Viscous Fingers: Quantitative Characterization of a Fluid Instability Phenomenon Nature", Vol 209, pp 141-144.

Personne P., Gayet, J.F., (1984), "Etude théorique et expérimentale en soufflerie du phénomène d'accrétion de givre sur les lignes électriques aériennes", J. Rech. Atmos., Vol 18, pp 263-279.